

CeIr₃Ge₇: a local moment antiferromagnetic metal with extremely low ordering temperature

Binod K. Rai¹, Jacintha Banda², Macy Stavinoha³, R. Borth², D.-J. Jang², Katherine A. Benavides⁴, D. A. Sokolov², Julia Y. Chan⁴, M. Nicklas², Manuel Brando², C.-L. Huang¹, and E. Morosan¹

¹*Department of Physics and Astronomy, Rice University, Houston, TX 77005 USA*

²*Max Planck Institute for Chemical Physics of Solids, Dresden, 01187 Germany*

³*Department of Chemistry, Rice University, Houston, TX 77005 USA*

⁴*Department of Chemistry & Biochemistry, University of Texas at Dallas, Richardson, TX 75080 USA*

(Dated: April 17, 2018)

CeIr₃Ge₇ is an antiferromagnetic metal with a remarkably low ordering temperature $T_N = 0.63$ K, while most Ce-based magnets order between 2 and 15 K. Thermodynamic and transport properties as a function of magnetic field or pressure do not show signatures of Kondo correlations, interaction competition, or frustration, as had been observed in a few antiferromagnets with comparably low or lower T_N . The averaged Weiss temperature measured below 10 K is comparable to T_N suggesting that the RKKY exchange coupling is very weak in this material. The unusually low T_N in CeIr₃Ge₇ can therefore be attributed to the large Ce-Ce bond length of about 5.7 Å, which is about 1.5 Å larger than in the most Ce-based intermetallic systems.

Compounds containing Ce or Yb ions have been studied extensively due to their diverse ground states originating from the competition between several energy scales. The competition between Ruderman-Kittel-Kasuya-Yosida (RKKY) exchange interaction and Kondo coupling give rise to intermediate valence behavior¹⁻⁴ or Kondo screening⁴⁻⁹ which, in turn, often result in unconventional superconductivity, non-Fermi liquid behavior, and quantum criticality^{7,10-13}. If the hybridization between *f* electrons and conduction electrons is very weak, the ground states of these systems are dictated by RKKY exchange interaction and crystal electric field (CEF) effects, resulting in long-range magnetic order.¹⁴⁻¹⁶ In the case of the Ce local moment metals without the Kondo effect, the ordering temperatures range from $T_C = 115$ K^{17,18} in ferromagnetic CeRh₃B₂, to $T_N = 2.75$ K¹⁹ in antiferromagnetic (AFM) CeSbTe, while much lower temperatures can be expected for the Yb analogues²⁰. Lower ordering temperatures in both Ce³⁺ and Yb³⁺ compounds could occur from any combination of effects including Kondo, competition between different exchange interactions, strong CEF anisotropy, or large distances between rare-earth ions (d_{R-R}) that minimize the RKKY exchange coupling J_{RKKY} . Compounds with low ordering temperatures often involve either weaker-than-RKKY exchange, as is the case in insulators, or multipolar order²¹, in which case the resulting order is almost always underlined by heavy fermion (HF) behavior. A remarkably low Néel temperature $T_N = 0.18$ K has been observed in the intermetallic compound Ce₄Pt₁₂Sn₂₅²². However, the peak around T_N in the magnetic specific heat extends well into the paramagnetic state, and this has been attributed to either the onset of Kondo screening or frustration.

Here we report the discovery of CeIr₃Ge₇, a new intermetallic compound without Kondo effect and no geometric frustration, with a remarkably low AFM ordering temperature $T_N = 0.63$ K. This is one of several $R =$ Ce or Yb compounds we recently discovered in the RT_3M_7

(1-3-7) class of compounds with $T =$ transition metal and $M =$ group 14 element^{9,23,24}, a family of rhombohedral intermetallics with the ScRh₃Si₇ structure type^{25,26}. The R sublattice forms a cubic structure, with nearest-neighbor d_{R-R} around 5.7 Å. Strong electron correlations in the Yb members of this family result in HF behavior and ferromagnetic or AFM ordering at temperatures as high as 7.5 K. Remarkably, CeIr₃Ge₇ is weakly correlated, and even with similar d_{R-R} , the ordering temperature is much smaller than in the HF Yb analogues. This seems uncommon when compared to other HF systems where the Yb compounds usually order at lower temperatures than the Ce counterparts, due to deeper localization of the 4*f* electron and the larger strength of the spin-orbit coupling in the former²⁰. Such a comparison could be tenuous since we neglect all the details of band structures. No frustration is present in CeIr₃Ge₇, as the Weiss temperature in the limit of absolute zero is close to T_N . This system is a good metal, with residual resistivity values $\rho_0 \sim 20$ $\mu\Omega$ cm and a residual resistivity ratio $RRR = \rho(300K)/\rho_0 \sim 5$. No Kondo correlations are apparent as most of the magnetic entropy is released below T_N . In the absence of Kondo effect or frustration, the low T_N in CeIr₃Ge₇ is attributed to the large distance d_{R-R} . This points to the potential of the 1-3-7 family to reveal Ce or Yb compounds with low ordering temperatures, which, in turn, may be easily tuned towards absolute zero transitions and quantum critical regimes.

CeIr₃Ge₇ crystallizes in the $R\bar{3}c$ rhombohedral ScRh₃Si₇ structure type^{25,26}. The very few 1-3-7 compounds known so far are RAu_3Ga_7 ($R =$ Gd-Yb)^{27,28}, non-magnetic RAu_3Al_7 ($R =$ Ce-Sm, Gd-Lu)²⁹, and magnetic Eu(Rh,Ir)₃Ge₇³⁰. Recently we discovered the first magnetic Ce and Yb 1-3-7 compounds. All of the newly discovered compounds were synthesized in single crystal form using a self-flux growth method^{31,32}, with details described elsewhere⁹. Single crystal x-ray diffraction measurements confirm the ScRh₃Si₇ structure type and verify the purity and stoichiometry of these com-

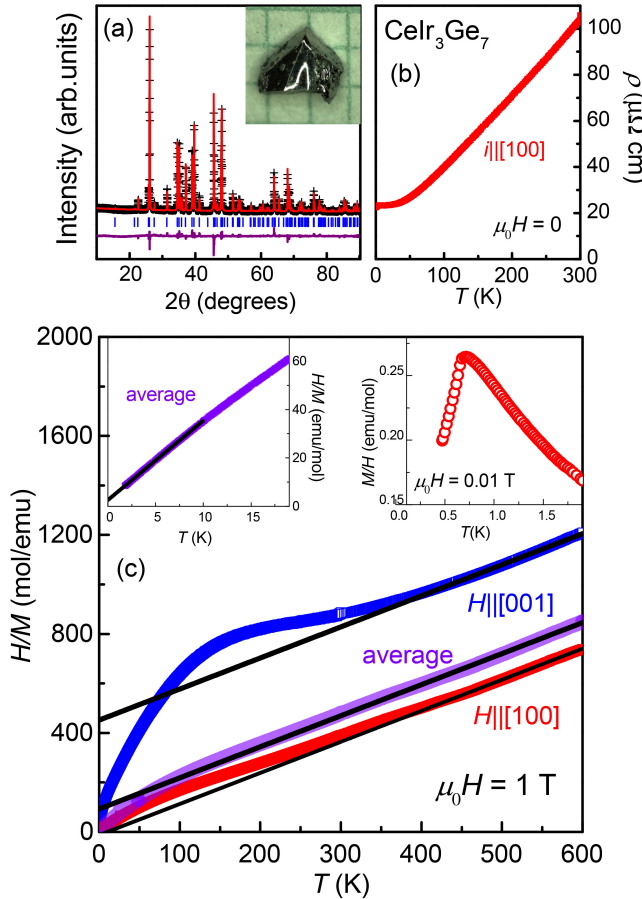


FIG. 1: (a) Room temperature (symbols) and calculated (red line) powder x-ray diffraction patterns of CeIr₃Ge₇, together with the expected peak positions (blue vertical lines) for space group $R\bar{3}c$ and lattice parameters $a = 7.8915(8)$ Å and $c = 20.788(6)$ Å. Violet curves are the difference between data and calculated patterns. Inset: crystal picture. (b) Zero-field resistivity with current parallel to the [100] axis. (c) Inverse magnetic susceptibility H/M vs. T for magnetic field $H \parallel [001]$ (blue), [100] (red), and a polycrystalline average (violet). Solid lines are high temperature Curie-Weiss fits, with Weiss temperatures of -360 K, -20 K and -100 K for $H \parallel [001]$, [100], and the polycrystalline average, respectively (see text). Left inset: the low-temperature H/M vs. T with a linear fit for the polycrystalline average. Right inset: the low-temperature M/H vs. T for $H \parallel [100]$.

pounds. The details of the x-ray diffraction and experimental methods are described in the Supplementary Material³³. A nonmagnetic analogue YIr₃Ge₇ polycrystalline sample was prepared by arc melting. Figure 1(a) shows a powder x-ray pattern and structural refinement for CeIr₃Ge₇ with a photo of a crystal shown in the inset. In this rhombohedral crystal structure, the R atoms form a cubic sublattice⁹, with the body diagonal of the cube parallel to the c axis of the equivalent hexagonal unit cell. Notably, the distances $d_{R-R} \sim 5.7$ Å are larger than in many magnetic R intermetallics, but do not change significantly for $R = \text{Ce}$ or Yb in the 1-3-7 structure.

This observation becomes most relevant when trying to explain the low ordering temperature $T_N = 0.63$ K in CeIr₃Ge₇. Several scenarios may in principle result in low T_N in Ce compounds, such as the Kondo effect, frustration or exchange coupling competition, weak exchange due to large $d_{\text{Ce-Ce}}$. The following discussion is based on evidence against most, if not all, of these scenarios in CeIr₃Ge₇, rendering this compound a unique non-Kondo metal with extremely low ordering temperature.

The $\mu_0 H = 0$ resistivity measurements (Fig. 1 (b)) show that CeIr₃Ge₇ is a good metal, with a RRR = 5 and residual resistivity $\rho_0 \sim 20 \mu\Omega\text{cm}$. However, upon cooling from room temperature, the resistivity is linear in temperature, and no signatures of Kondo correlations are apparent. The lack of Kondo effect will be further corroborated by the specific heat data shown later. For now, we turn to the magnetic susceptibility measured along ($H \parallel [001]$) and perpendicular ($H \parallel [100]$) to the c axis of the equivalent hexagonal unit cell. The inverse susceptibility H/M (Fig. 1(c)), measured up to 600 K, reveals large easy-plane CEF anisotropy. The average susceptibility is calculated as $M_{\text{ave}} = (M_{001} + 2M_{100})/3$. Fits to the Curie-Weiss law at high temperatures are shown in solid black lines. The experimental effective moment $\mu_{\text{eff}}^{\text{exp}}$ extracted from the fit of the average susceptibility (violet, Fig. 1(c)) is $\mu_{\text{eff}}^{\text{exp}} = 2.52 \mu_B/\text{Ce}^{3+}$, pointing to localized, trivalent Ce ions in CeIr₃Ge₇, since the expected Ce³⁺ calculated effective moment $\mu_{\text{eff}}^{\text{calc}} = 2.52 \mu_B/\text{Ce}^{3+}$ is virtually identical to the experimental value. The negative Weiss temperatures indicate AFM correlations. The H/M data deviate from the Curie-Weiss law due to CEF splitting of the $J = 5/2$ multiplet. The deviation indicates a separation of the first excited CEF doublet of ~ 400 K, consistent with the CEF calculations which will be reported elsewhere⁵⁵.

In the $T \rightarrow 0$ limit, the inverse susceptibility intercept with the temperature axis is around -2 K for M_{ave} (left inset, Fig. 1(c)), comparable to the low ordering temperature $T_N \sim 0.6$ K indicated by the cusp in M/H vs. T for $H \parallel [001]$ (right inset, Fig. 1(c)). These observations can be reconciled by considering the Weiss temperatures at $T \rightarrow 0$ to reflect the exchange coupling J_{ex} , which consequently indicates that J_{ex} is inherently small in CeIr₃Ge₇. At high T , the Weiss temperatures are enhanced by the large CEF effects. We show the $M(H)$ isotherms in Fig. 2 for $H \parallel [100]$ (red symbols) and $H \parallel [001]$ (blue symbols), in the ordered state $T = 0.5$ K (full symbols) and the paramagnetic state $T = 1.8$ K (open symbols). A Brillouin function at 1.8 K along [100] direction, shown as a solid black line in Fig. 2, agrees very well with the experimental data, indicating that the measured magnetization mostly comes from isolated paramagnetic moments. The $M(H)$ measurements confirm the in-plane and out-of-plane magnetic anisotropies, and, more quantitatively, are in good agreement with the calculated moments of $0.91 \mu_B/\text{Ce}$ and $0.33 \mu_B/\text{Ce}$ along the easy ([100]) and hard ([001]) directions, respectively⁵⁵. A magnetic field close to $\mu_0 H = 1.7$

T is required for saturation in the easy direction (squares, Fig. 2), while a linear extrapolation of $M(H \parallel [001])$ suggests a magnetic field in excess of 20 T is needed to reach saturation in the hard direction.

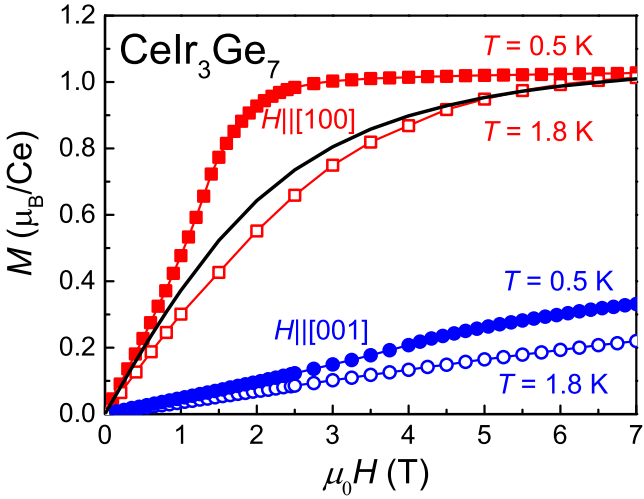


FIG. 2: CeIr_3Ge_7 M vs. H isotherms for $T = 0.5$ K (full symbols) and 1.8 K (open symbols) for $H \parallel [001]$ (blue circles) and $H \parallel [100]$ (red squares). The solid black line is the Brillouin function for $T = 1.8$ K, with a scaled magnitude.

Because of this extremely large anisotropy, and the large magnetic field scale in the hard ($[001]$) direction, we focus next only on the field dependence of the ordering temperature T_N for the easy direction $H \parallel [100]$, as illustrated by the M/H and specific heat C_p data in Fig. 3. For AFM systems, a peak in C_p at T_N is expected to correspond to a peak in $d(MT)/dT^{56}$, and this is illustrated for $\mu_0H = 0.01$ T (solid line, right axis) in Fig. 3(a). Both ambient pressure M/H and C_p measurements (3(a-b)) reveal the expected suppression of T_N with increasing H , such that above $\mu_0H = 1.7$ T, no peak can be resolved above 350 mK. Consistent with the zero field resistivity data in Fig. 1(b), the specific heat data show an entropy release of $\sim 2/3$ Rln2 at T_N (solid line, right axis in Fig. 3c), reaffirming the absence of both Kondo effect and strong correlations in CeIr_3Ge_7 . To further rule out the presence of Kondo screening, one can consider the analysis by de Jongh and Miedema⁵⁷, which shows that an entropy release of 15%-40% of Rln2 above T_N can be expected in AFM systems around T_N . Indeed this is reflected in the $H = 0$ magnetic entropy plot of CeIr_3Ge_7 in Fig. 3(b) (black line). Furthermore, the same model indicates that the C_p contribution from Kondo is much weaker than that from classical intersite fluctuations. Within a Heisenberg model, one expects that, far above T_N , the leading term in $C_p(T)$ is proportional to $1/T^2$, i.e., $C_p/T \sim 1/T^3$. Upon applying a magnetic field (Fig. 3(b)), the dispersion of the magnons changes. In an AFM system the energy gap at $\mathbf{Q} = 0$ decreases and disappears at $\mu_0H = \mu_0H_c \approx 1.7$ T. This results in a large increase of the low energy magnon-like

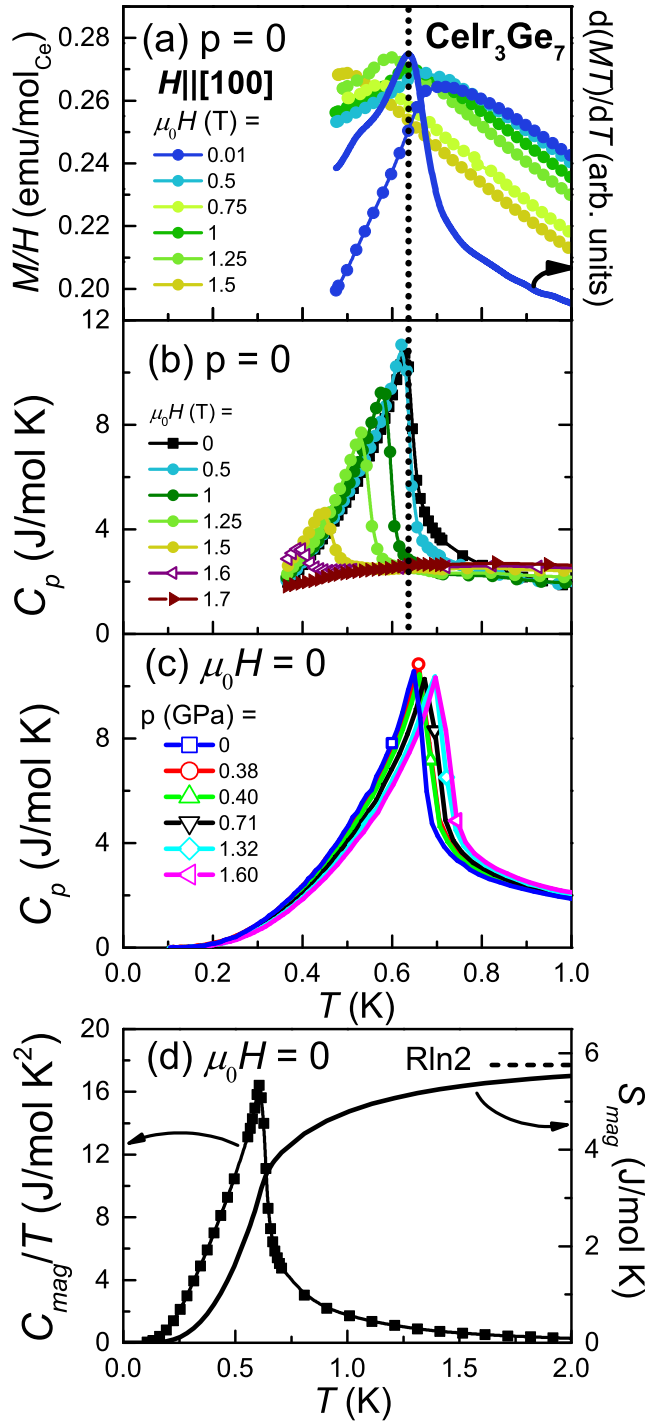


FIG. 3: (a) Left axis: magnetic susceptibility M/H vs. T . Right axis: $d(MT)/dT$ vs. T (solid line) for $\mu_0H = 0.01$ T. (b) Left axis: specific heat C_p vs. T (symbols) for different magnetic fields. The vertical dashed line through (a) to (b) marks T_N at zero field. (c) Temperature dependent specific heat for different pressures. (d) Left axis: magnetic contribution to the specific heat C_{mag}/T vs. T . Right axis: magnetic entropy S_{mag} vs. T . $C_{mag}/T = C_p/T(\text{CeIr}_3\text{Ge}_7) - C_p/T(\text{YIr}_3\text{Ge}_7)$, where YIr_3Ge_7 is a nonmagnetic analogue.

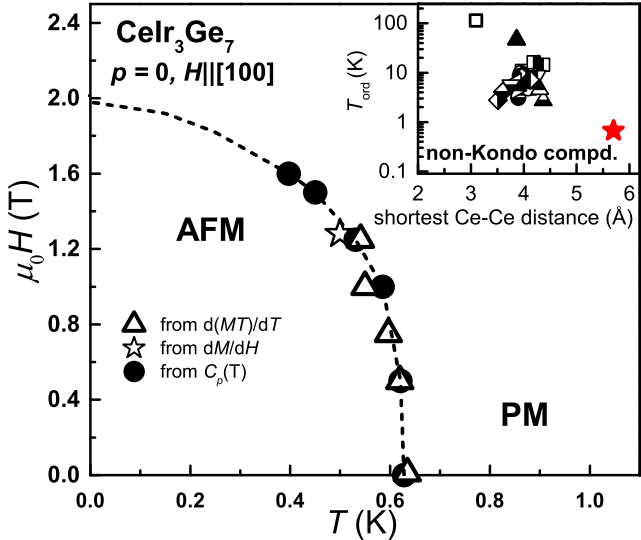


FIG. 4: $T - H$ phase diagram of CeIr_3Ge_7 at ambient pressure with $H \parallel [100]$. Inset: ordering temperature T_{ord} vs. the shortest Ce-Ce distance in known intermetallic non-Kondo Ce compounds. Different symbols refer to different compounds tabulated in Supplemental Material³⁴⁻⁵⁴.

excitations, which, in turn, shows up as a strong increase of C_p near and above T_N . For $H > H_c$ (full right triangles, Fig. 3(b)), a gap reopens in the magnon excitation spectra, and the specific heat evolves towards a broad anomaly related to the dominant Zeeman splitting.

Complementary to the field dependence, the pressure dependence of the specific heat (Fig. 3(c)) underlines the conclusion of small or negligible Kondo correlations: T_N increases linearly with pressures up to 1.6 GPa at a rate of $dT_N/dp = 3.71 \times 10^{-2}$ K/GPa. The increase of T_N under pressure, if only being ascribed to a volume effect, can be understood in the framework of the Doniach phase diagram⁵⁸. The positive, yet very small, slope of $T_N(p)$ for CeIr_3Ge_7 suggests that this compound is located at far left of $T_N^{\text{max}}(J_{\text{ex}})$ in the Doniach diagram⁵⁸. The $T - H$ phase diagram in Fig. 4 summarizes the T_N dependence on field at ambient pressure.

Among non-Kondo magnetic Ce compounds, CeIr_3Ge_7 stands out (red in inset of Fig. 4) together with CeRh_3B_2 (open square in inset of Fig. 4). The latter orders ferromagnetically with a remarkably large Curie temperature (~ 115 K) due to the enhancement of the exchange interaction from the $J = 7/2$ multiplet, despite short $d_{\text{Ce-Ce}} = 3.096$ Å¹⁸. Of note is the compound $\text{Ce}_4\text{Pt}_{12}\text{Sn}_{25}$ (Ref. 22), which appears to have a record low $T_N = 0.18$ K and represents a Kondo lattice in the small exchange limit of the Doniach phase diagram. In

this case, however, the extremely low T_N is a result of the large $d_{\text{Ce-Ce}} \sim 6.14$ Å, weak Kondo screening just above T_N (marked by a tail in the magnetic specific heat peak just above the ordering), and weak geometric frustration due to the three-fold point symmetry of the Ce site⁵⁹. Except for the large $d_{\text{Ce-Ce}} \sim 5.7$ Å, none of these effects are at play in CeIr_3Ge_7 : the low temperature Weiss temperatures (Fig. 1(c) inset) are comparable with T_N , ruling out significant frustration effects; the specific heat peak (Fig. 3(b)) terminates abruptly at T_N , and $\rho(T)$ decreases linearly with temperature before it levels off at ρ_0 at the lowest temperatures (Fig. 1(b)), therefore no Kondo screening signatures are apparent. Ce and Yb magnetic (trivalent) compounds are often thought as electron-hole analogues. In metals, the exchange coupling decreases from Ce to Yb, and therefore larger ordering temperatures are expected in the former compared to the latter. So, in the absence of Kondo effect or frustration, CeIr_3Ge_7 should have a magnetic ordering temperature larger than its Yb analogue. What we find is that YbIr_3Ge_7 is in fact an HF ferromagnet²⁴, and this should further suppress the magnetic order to temperatures well below $T_N(\text{Ce})$. Instead, the Curie temperature for this HF ferromagnet is large $T_C \sim 2.4$ K, despite the nearly identical d_{R-R} in both the Ce and Yb analogues. This may reflect that the details of the band structure near the Fermi surface of Ce and Yb analogues plays an important role of magnetism. In summary, CeIr_3Ge_7 in particular and more generally the 1-3-7 family of magnetic compounds provide a fertile ground for exploring magnetic correlations and the competition among various energy scales (RKKY, Kondo, CEF) which could result in novel quantum critical regimes. In addition, their rhombohedral structure allows for very weak coupling between the Ce atoms in a good metallic environment, similar to what was observed in YbPt_2Sn ⁶⁰. This is an excellent precondition for metallic magnets that can be used for adiabatic demagnetization cooling below 2 K, instead of insulating paramagnetic salts.

Acknowledgements We thank J. Simone, J. D. Thompson, C. Geibel, and W. Hu for fruitful discussions. Work at Rice University was supported by the Gordon and Betty Moore Foundation EPiQS Initiative through grant GBMF 4417. The work at University of Texas at Dallas was supported by nsf-dmr 1700030. This research is funded in part by a QuanEmX grant from ICAM and the Gordon and Betty Moore Foundation through Grant GBMF5305 to Binod Rai. EM acknowledges travel support to Max Planck Institute in Dresden, Germany from the Alexander von Humboldt Foundation Fellowship for Experienced Researchers.

¹ R. Currat, R. G. Lloyd, P. W. Mitchell, A. P. Murani, and J. W. Ross, *Physica B* **156**, 812 (1989).

² T. Mazet, D. Malterre, M. Francois, C. Dallera, M. Grioni, and G. Monaco, *Phys. Rev. Lett.*, **111** 096402 (2013).

³ Binod K. Rai and E. Morosan, *APL Mater.* **03**, 041511 (2015).

⁴ Binod K. Rai, Iain W. H. Oswald, Julia Y. Chan, and E. Morosan, *Phys. Rev. B* **93**, 035101 (2016).

⁵ E. Morosan, S. L. Bud'ko, Y. A. Mozhariivskyj, P. C. Canfield, *Phys. Rev. B* **73**, 174432 (2006).

⁶ P. Gegenwart, T. Westerkamp, Krellner, Y. Tokiwa, S. Paschen, C. Geibel, F. Steglich, E. Abrahams, and Q. Si, *Science* **315**, 969 (2007).

⁷ Johnpierre Paglione, T. A. Sayles, P.-C. Ho, J. R. Jeffries, and M. B. Maple, *Nat. Phys.* **3**, 703 (2007).

⁸ Rai et al., unpublished.

⁹ Rai et al., arXiv:1803.04013.

¹⁰ H. v. Löhneysen, A. Rosch, M. Vojta, and P. Wöfle, *Rev. Mod. Phys.* **79**, 1015 (2007).

¹¹ Erwin Schuberth, Marc Tippmann, Lucia Steinke, Stefan Lausberg, Alexander Steppke, Manuel Brando, Cornelius Krellner, Christoph Geibel, Rong Yu, Qimiao Si, and Frank Steglich, *Science* **351**, 485 (2016).

¹² J. Custers, P. Gegenwart, H. Wilhelm, K. Neumaier, Y. Tokiwa, O. Trovarelli, C. Geibel, F. Steglich, C. Pépin, and P. Coleman, *Nature* **424**, 524 (2003).

¹³ Alexander Steppke, Robert Küchler, Stefan Lausberg, Edit Lengyel, Lucia Steinke, Robert Borth, Thomas Lühmann, Cornelius Krellner, Michael Nicklas, Christoph Geibel, Frank Steglich, and Manuel Brando, *Science* **339**, 933 (2013).

¹⁴ V. Fritsch, P. Pfundstein, P. Schweiss, E. Kampert, B. Pilawa, and H. v. Löhneysen, *Phys. Rev. B* **84**, 10446 (2011).

¹⁵ C. L. Huang, V. Fritsch, W. Kittler, and H. v. Löhneysen, *Phys. Rev. B* **86**, 214401 (2012).

¹⁶ M. O. Ajeesh, T. Shang, W. B. Jiang, W. Xie, R. D. dos Reis, M. Smidman, C. Geibel, H. Q. Yuan, and M. Nicklas, *Scientific Report* **7**, 7338 (2017).

¹⁷ S K Dhar, S K Malik and R Vijayaraghavan, *J. Phys. C: Solid State Phys.* **14**, L321 (1981).

¹⁸ F Givord, J-X Boucherle, R-M Galéra, G Fillion, and P Lejay, *J. Phys.: Condens. Matter* **19**, 356208 (2007).

¹⁹ Leslie M. Schoop, Andreas Topp, Judith Lippmann, Fabio Orlandi, Lukas Müchler, Maia G. Vergniory, Yan Sun, Andreas W. Rost, Viola Duppel, Maxim Krivenkov, Shweta Sheoran, Pascal Manuel, Andrei Varykhalov, Binghai Yan, Reinhard K. Kremer, Christian R. Ast, and Bettina V. Lotsch *Sci. Adv.* **4**, eaar2317 (2018).

²⁰ J. Flouquet and H. Harima *arXiv*: 0910.3110.

²¹ P. Y. Portnichenko, S. Paschen, A. Prokofiev, M. Vojta, A. S. Cameron, J.-M. Mignot, A. Ivanov, and D. S. Inosov, *Phys. Rev. B* **94**, 245132 (2016).

²² Nobuyuki Kurita, Han-Oh Lee, Yoshi Tokiwa, Cornelius F. Miclea, Eric D. Bauer, Filip Ronning, J. D. Thompson, Zachary Fisk, Pei-Chun Ho, M. Brian Maple, Pinaki Sengupta, Ilya Vekhter, and Roman Movshovich, *Phys. Rev. B* **82**, 174426 (2010).

²³ Magnetic properties of RRh_3Si_7 ($R = Gd$ -Yb) single crystals: Binod K. Rai, Macy Stavinoha, Katherine Benavides, Julia Y. Chan, and E. Morosan, *in preparation*.

²⁴ Binod K. Rai, Macy Stavinoha, Daniel Hafner, Chien-Lung Huang, M. Brando, and E. Morosan, *in preparation*.

²⁵ B. Chabot, N. Engel, and E. Parthé, *Acta Crystallogr., B* **37**, 671 (1981).

²⁶ P. Lorenz, and W. Jung, *Acta Cryst.* **E62**, i173 (2006).

²⁷ G. Cordier, and Ch. Dietrich, *Zeitschrift für Kristallographie - Crystalline Materials.*, **211**, 118 (1996).

²⁸ Yury Verbovetsky, *Chem. Met. Alloys* **7**, 42 (2014).

²⁹ S. E. Latt Turner, D. Bilc, J. R. Ireland, C. R. Kannewurf, S. D. Mahanti, and M. G. Kanatzidis, *J. Solid State Chem.* **170**, 48 (2003).

³⁰ M. Falmbigl, F. Kneidinger, A. Grytsiv, H. Michor, H. Müller, P. Rogl, E. Bauer, G. Hilscher, G. Giester, *Intermetallics* **42**, 45 (2013).

³¹ J. P. Remeika, G. P. Espinosa, A. S. Cooper, H. Barz, J. M. Rowell, D. B. McWhan, J. M. Vandenberg, D. E. Moncton, Z. Fisk, L. D. Woolf, H. C. Hamaker, M. B. Maple, G. Shirane, and W. Thomlinson, *Solid State Comm.* **34**, 923 (1980).

³² Binod K. Rai, Iain W. H. Oswald, J. K. Wang, G. T. McCandless, J. Y. Chan, and E. Morosan, *Chem. Mater.* **27**, 2494 (2015).

³³ See Supplemental Material at [URL will be inserted by publisher], which includes Refs. 34–54, for single-crystal x-ray analysis and a summary of non-heavy-fermion Ce-based compounds.

³⁴ M. Nicklas, in: *Strongly Correlated Systems Experimental Techniques*, edited by A. Avella and F. Mancini, Springer Series in Solid-State Sciences, Vol. 180 (Springer, Berlin, Heidelberg, 2015), pp. 173204.

³⁵ G.-F. von Blanckenhagen and G.R. Stewart, *Solid State Commun.* **108**, 535 (1998)

³⁶ R. Kraft, R. Pöttgen, and D. Kaczorowski, *Chem. Mater.* **15**, 2998 (2003)

³⁷ B. M. Mhlungu and A. M. Strydom, *Physica B* **403**, 862 (2008)

³⁸ M. O. Ajeesh, T. Shang, W. B. Jiang, W. Xie, R. D. dos Reis, M. Smidman, C. Geibel, H. Q. Yuan, and M. Nicklas, *Sci. Rep.* **7**, 7338 (2017)

³⁹ C. L. Huang, V. Fritsch, B. Pilawa, C. C. Yang, M. Merz, and H. v. Löhneysen, *Phys. Rev. B* **91**, 144413 (2015)

⁴⁰ M. Lenkewitz, S. Corsépius, and G.R. Stewart, *J. Alloys Compd.*, **241**, 121 (1996)

⁴¹ A. Grytsiv, E. Bauer, St. Berger, G. Hilscher, H. Michor, Ch. Paul, P. Rogl, A. Daoud-Aladine, L. Keller, T. Roisnel, and H. Noel, *J. Phys: Condens. Matter* **15**, 3053 (2003)

⁴² D. Gignoux, D. Schmitt, and M. Zerguine, *Solid State Commun.* **58**, 559 (1986)

⁴³ Y. Oner, O. Kamer, Joseph H. Ross Jr., C.S. Lue, and Y.K. Kuo, *Solid State Commun.* **136**, 533 (2005)

⁴⁴ C. L. Huang, V. Fritsch, W. Kittler, and H. v. Löhneysen, *Phys. Rev. B* **86**, 214401 (2012)

⁴⁵ M. Klicpera, S. Mašková, M. Diviš, P. Javorský, and L. Havela, *J Magn. Magn. Mater.* **404**, 250 (2016)

⁴⁶ A. Loidl, K. Knorr, G. Knopp, A. Krimmel, R. Caspary, A. Böhm, G. Sparn, C. Geibel, F. Steglich, and A. P. Murani, *Phys. Rev. B* **46**, 9341 (1992)

⁴⁷ Yongkang Luo, Jinke Bao, Chenyi Shen, Jieke Han, Xiaojun Yang, Chen Lv, Yuke Li, Wenhe Jiao, Bingqi Si, Chunmu Feng, Jianhui Dai, Guanghan Cao, and Zhu-an Xu, *Phys. Rev. B*, **86** 245130 (2012)

⁴⁸ H. Nakotte, E. Brück, K. Prokes, J.H.V.J. Brabers, F.R. de Boer, L. Havela, K.H.J. Buschow, and Yang Fu-ming, *J. Alloys Compd.* **207/208**, **245** (1994)

⁴⁹ J. Ph. Schillé, I. Poinsot, C. Giorgetti, P. Sainctavit, G. Fischer, C. Brouder, F. Bertran, M. Finazzi, C. Godart, E. Dartige, J.P. Kappler, and G. Krill, *Physica B* **199&200** 563 (1994)

⁵⁰ K. Shigetoh, A. Ishida, Y. Ayabe, T. Onimaru, K. Umeo, Y. Muro, K. Motoya, M. Sera, and T. Takabatake, *Phys. Rev. B* **76**, 184429 (2007)

⁵¹ R. E. Baumbach, T. Shang, M. Torrez, F. Ronning, J. D.

Thompson, and E. D. Bauer, *J. Phys.: Condens. Matter* **24**, 185702 (2012)

⁵² S. A. Shaheen, *J. Appl. Phys.* **63**, 3411 (1988)

⁵³ A. Thamizhavel, R. Kulkarni, and S. K. Dhar, *Phys. Rev. B* **75**, 144426 (2007)

⁵⁴ J.G. Sereni, P. Pedrazzini, M. Gómez Berisso, A. Chacoma, S. Encina, T. Gruner, N. Caroca-Canales, and C. Geibel, *J. Phys.: Conf. Ser.* **592**, 012005 (2015)

⁵⁵ Jacintha Banda, Binod K. Rai, E. Morosan, C. Geibel, and M. Brando, *in preparation*.

⁵⁶ Michael E. Fisher, *Philos. Mag.* **7**, 1731 (1962).

⁵⁷ L. J. DE Jongh and A. R. Miedema, *Adv. Phys.* **23**, 1 (1974).

⁵⁸ S. Doniach, *Physica* **91B**, 231 (1977).

⁵⁹ B D White, D Yazici, P-C Ho, N Kanchanavatee, N Pouse, Y Fang, A J Breindel, A J Friedman and M B Maple, *J. Phys.: Condens. Matter* **27**, 315602 (2015).

⁶⁰ D. Jong, T. Gruner, A. Steppke, K. Mitsumoto, C. Geibel, and M. Brando, *Nat. Commun.* **6**:8680 (2015).